

In this study, the causes and mechanisms of thermal distortion and quenching crack and the effects of kinds of cooling methods and cooling conditions of reverse transformation treatment were analyzed in order to prevent these troubles by the model of metallo-thermo-mechanics (5), (6). The cooling methods considered in these analyses were immersion cooling, spray cooling and mist-spray cooling.

ANALYSIS METHOD

ANALYSIS MODEL

Since the distribution of temperature and stress/strain and their transition and behavior of phase transformation affect mutually during third cooling, analyses combined distortion analysis with heat transfer analysis and analysis of phase transformation behavior are necessary to examine thermal distortion and stress generation considering these mutual effects. Therefore, the behavior of thermal distortion and stress generation were analyzed by the model of metallo-thermo-mechanics shown in Fig.1(5), (6): COSMAP (7) in this study. Thermo-elastic-plastic analysis, analysis of heat transfer and analysis about transformation behavior are combined in this model considering of thermal shrinkage and expansion, shrinkage and expansion accompanying transformation. The effects of cooling methods and cooling conditions on the behavior of thermal distortion and stress generation were studied by this model.

tion analysis with heat transfer analysis and analysis of phase transformation behavior are necessary to examine thermal distortion and stress generation considering these mutual effects. Therefore, the behavior of thermal distortion and stress generation were analyzed by the model of metallo-thermo-mechanics shown in Fig.1(5), (6): COSMAP (7) in this study. Thermo-elastic-plastic analysis, analysis of heat transfer and analysis about transformation behavior are combined in this model considering of thermal shrinkage and expansion, shrinkage and expansion accompanying transformation. The effects of cooling methods and cooling conditions on the behavior of thermal distortion and stress generation were studied by this model.

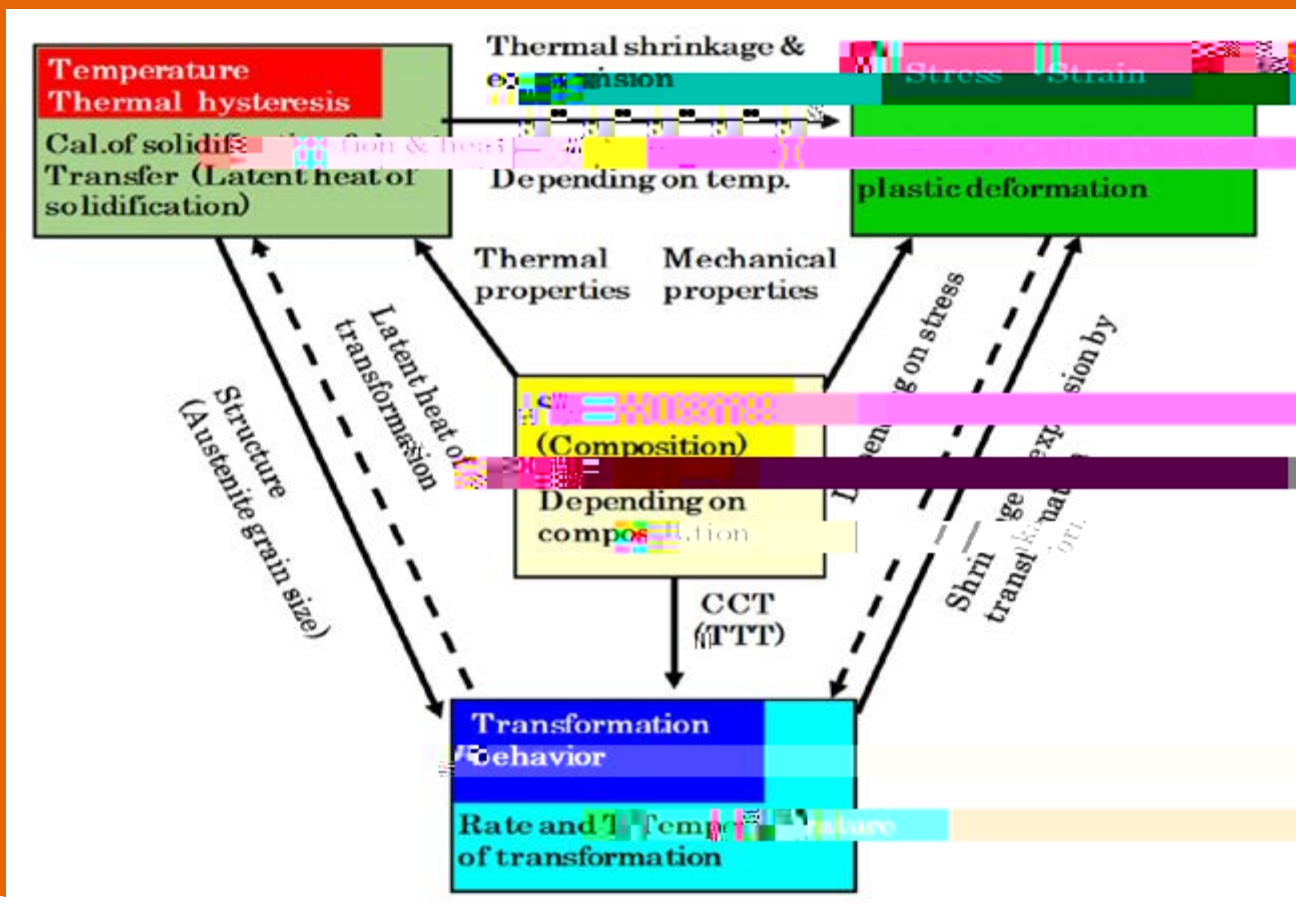


Fig.1 – Schematic view of the model of metallo-thermo-mechanics. (5)

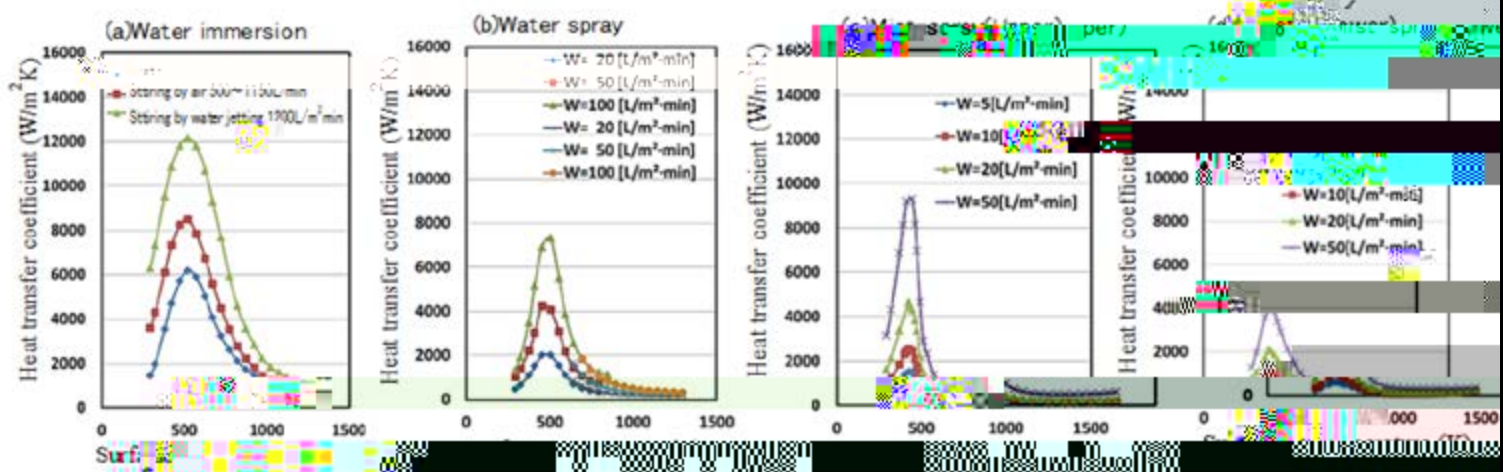
ANALYSIS CONDITIONS

The analyses were performed using a finite element method two-dimensional model for total cross section of a bloom having a square cross section of 200 mm (thickness) x 200 mm (width). The analyzed steel type was case hardening steel

SCr420(JIS), and the transformation behavior of this steel type was estimated in consideration of the CCT diagram measured in a coarse austenite structure similar to that of bloom as cast continuously (8).

In these calculations, the solidification calculation was not

performed, following cooling at 1123K, and cooling of the surface layer of the specimen into a ferrite-pearlite structure. The calculation was performed until the volume fraction of ferrite came less than 10%, assuming a cooling rate of 10 K/min and the effective cross-sectional area. The kinds of cooling were immersion, water spray, and water jetting at a water discharge rate of 100 L/min (cooling when the specimen is immersed in water). The relationship between the heat transfer coefficient and the distance from the surface is shown in Fig.2 (9).



Fig

RESULTS AND DISCUSSION

The cooling time required for the refinement of austenite grains in the surface layer of the bloom within a range of 10 mm by the reverse transformation treatment for various cooling methods and cooling conditions was clarified by the calculations. Fig. 3 is a bar graph showing the results of estimated the cooling time required for refining austenite grains. The required cooling time was determined as a time at which the volume fraction of austenite was 0.1 or less within a range of 10 mm from the surface of the bloom. As shown in this figure, the required cooling

time decreased with the increase of the cooling strength together with the uniform $T_w = 0 - 1.667 T_d$ [(togTh32lrPu9ume fra

The effects of the geometry of the block on the cooling curves were studied using finite element mechanics. As shown in Figure 1, the contour diagrams of the bainite and martensite volume fraction during the cooling process are shown in Figure 2. The section of the block is 40 times the thickness of the plate by cooling. The colors in the figure represent the volume fraction. In the case of the spray cooling, the transfer coefficient is 10000 W/m²·K.

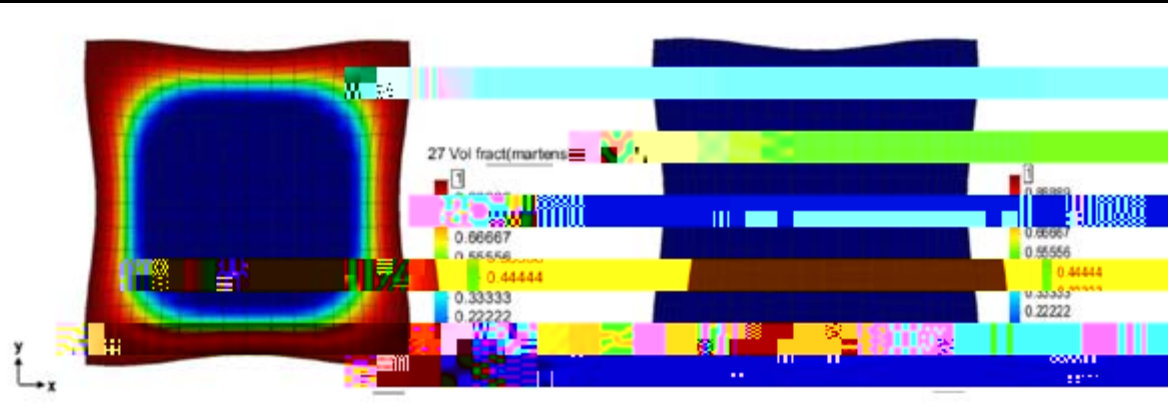


Fig. 1

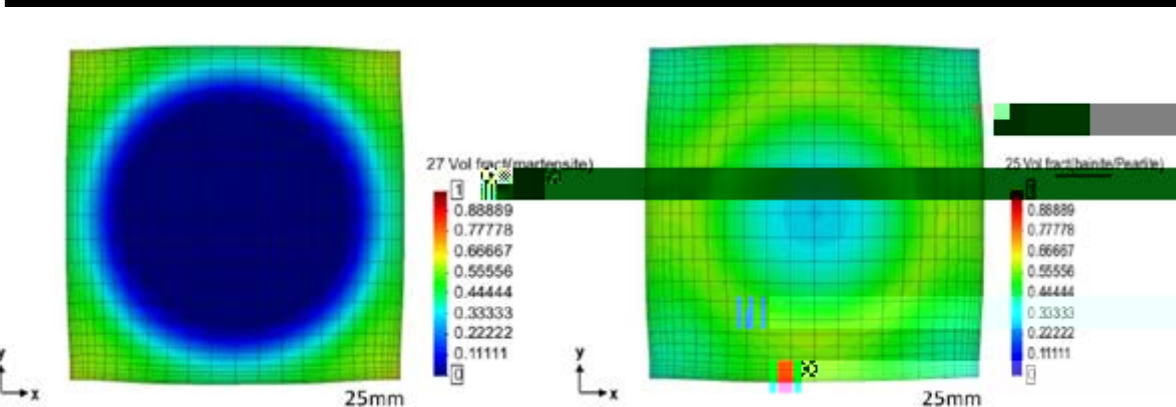


Fig. 2

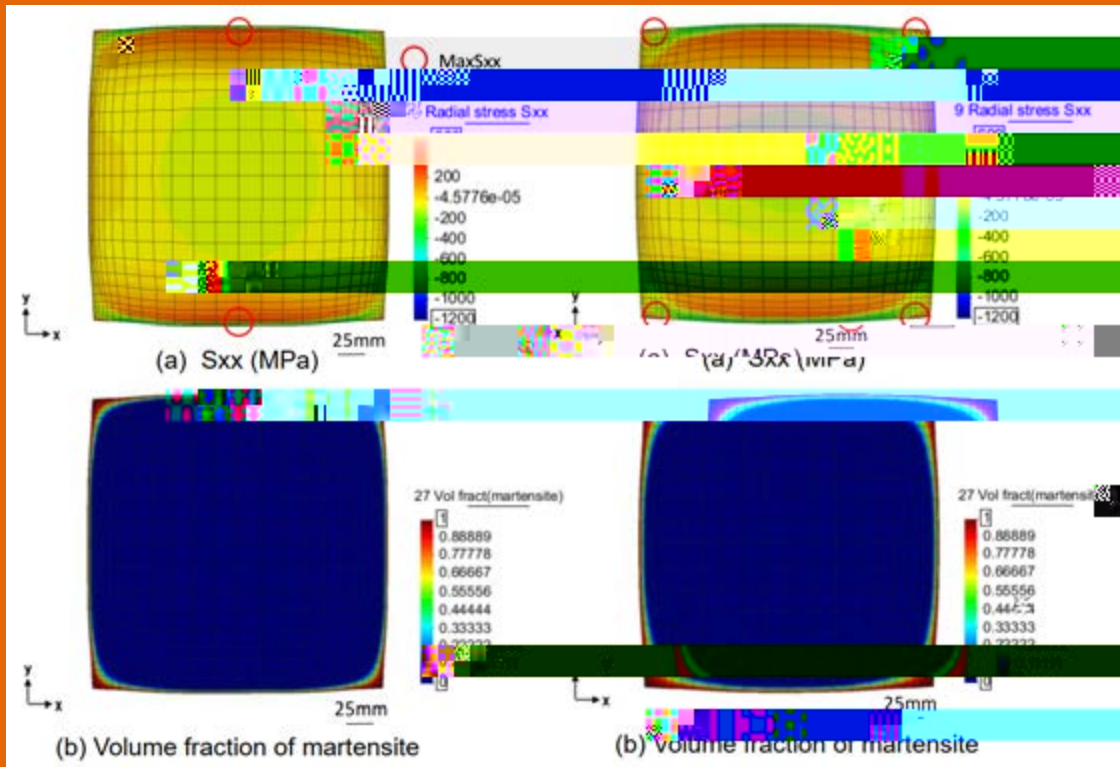
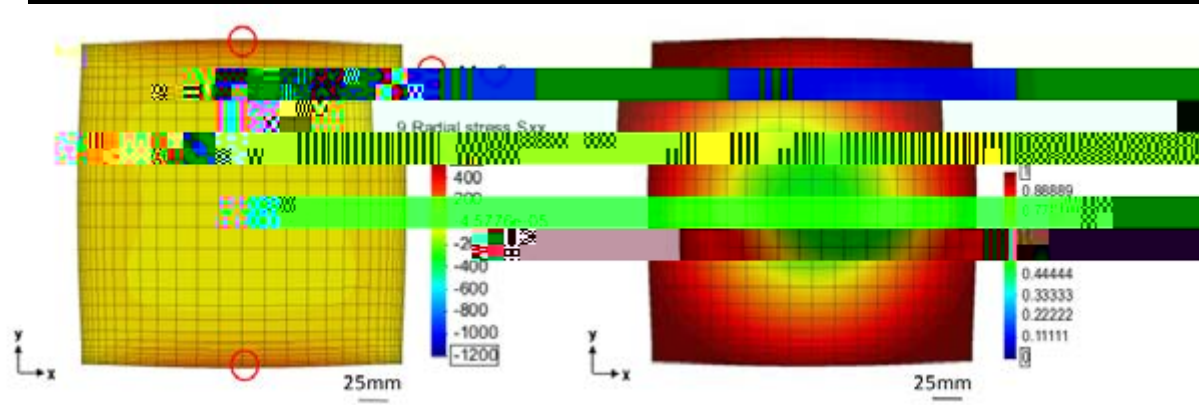


Fig.10 – Distribution of S_{xx} and volume fraction of martensite when S_{xx} is maximum during uniform immersion cooling. (Water jet stirring)

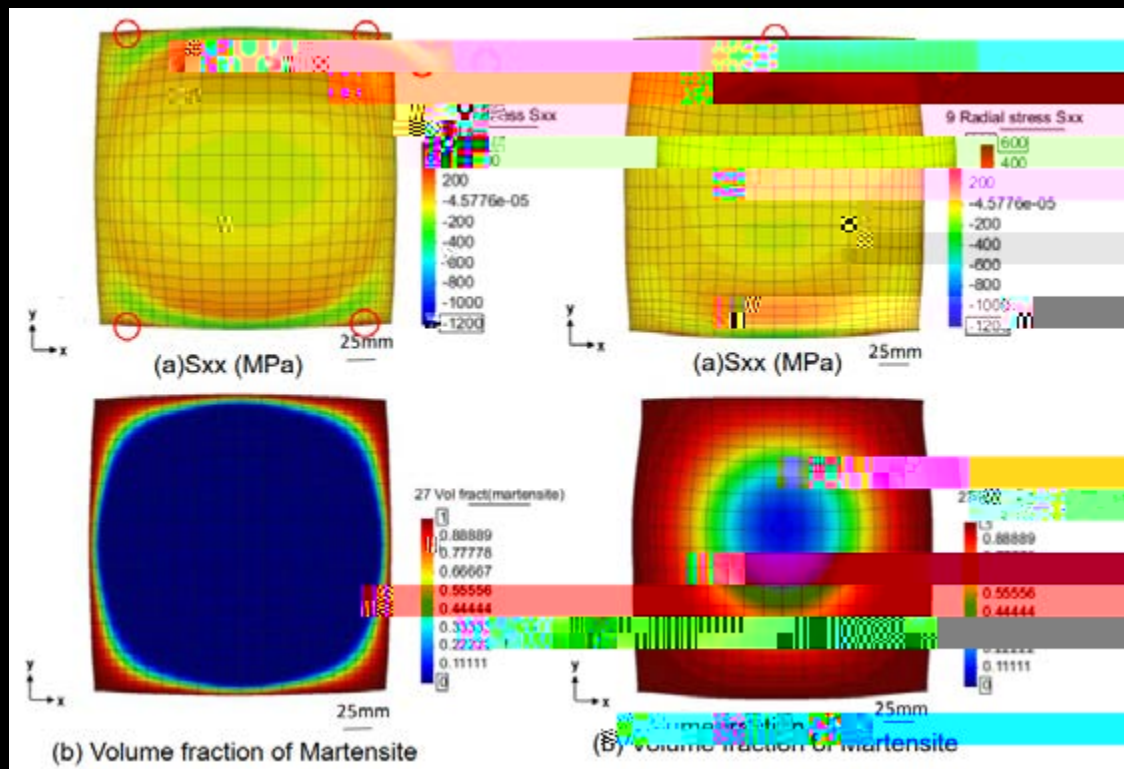
Fig.11 – Distribution of S_{xx} and volume fraction of martensite when S_{xx} is maximum during uniform immersion cooling. (Air stirring)

From the viewpoint of the prevention of the occurrence of quenching cracks, the behavior of stress generation in the cooling process by each cooling method was analyzed. Fig.10(a) and Fig.11(a) show the distributions of normal stress S_{xx} in the cross section of bloom in the case of uniform immersion cooling with water jet stirring and air stirring, when the stress S_{xx} during the cooling is maximum. Fig.10(b) and Fig.11(b) show the distributions of martensite volume fraction in the cross section at that time. The S_{xx} became maximum in the position indicated by the circle. In these cases of uniform immersion cooling, the amount generated bainite and pearlite phase is very small, and it is considered that the transformation expansion due to martensitic transformation near the surface of bloom and thermal stress cause the generation of maximum S_{xx} in these cases. In the case of immersion cooling with water jet stirring (Fig.10), the S_{xx} became maximum in the austenitic phase region just below the surface at the center of the surface. It was seemed that the

stress S_{xx} became the maximum just below the center of the surface, because the austenitic phase region just below the surface at the width center was pulled in the bloom width direction by the expansion due to martensitic transformation at the surrounding surface. On the other hand, in the case of immersion cooling with air stirring (Fig.11), the surface layer at the off-corner was pulled in the bloom width direction due to the progress of martensitic transformation inside the cross section of the corner. It is considered that the maximum stress S_{xx} occurred at the position, because of the martensitic transformation, the effect of thermal shrinkage and the large deformation resistance at the region caused by the low temperature.



F



layers and increased S_{xx} at the surface.

When the water density on the bloom upper surface side is 20 ($l/(m^2 \cdot \text{min})$), and the other three surfaces are cooled by spray at 100 ($l/(m^2 \cdot \text{min})$), distribution of S_{xx} and martensite volume fraction in the cross section of bloom are shown in Fig.14 in comparison with the case of cooling uniformly on all four sides with water density of 100 ($l/(m^2 \cdot \text{min})$)(Fig.13). In the case of uniform spray cooling with 100 ($l/(m^2 \cdot \text{min})$) shown in Fig.13, the maximum S_{xx} occurred on the off-corner surface due to expansion accompanying martensitic transformation at inside near the corner. In the non-uniform spray cooling (Fig.14), the upper surface layer whose temperature is higher than the other three surface layers is pulled due to martensitic transformation inside the cross section and the thermal shrinkage caused by constraint from the side surface of which temperature is lower. For the above reasons, it was found that the largest S_{xx} occurred at the center of the width of the upper surface in this case.

Compared with uniform cooling, in non-uniform cooling, the position, timing, and mechanism at which the ma-

ximum S_{xx} occurs differ greatly, and the maximum S_{xx} greatly increased in the case of non-uniform cooling with strong cooling intensity.

The maximum S_{xx} during cooling in various cooling methods and conditions is shown in the bar graph of Fig.15. In the uniform immersion cooling, the maximum S_{xx} was almost constant regardless of the stirring power of the immersion bath. In the uniform cooling with spray and mist-spray, S_{xx} decreased as the water density decreased. In this study, in spray cooling and mist cooling, there are some cases where non-uniform cooling significantly increased the maximum S_{xx} in comparison with uniform cooling.

From the results shown in this figure, it was found that spray cooling or mist cooling at a low water density of about 20 ($l/(m^2 \cdot \text{min})$) was preferable to reduce the stress of S_{xx} etc. It was estimated that it was important for decrease of stress and prevention of quenching crack occurrence to reduce the variation in cooling strength between surfaces of bloom.

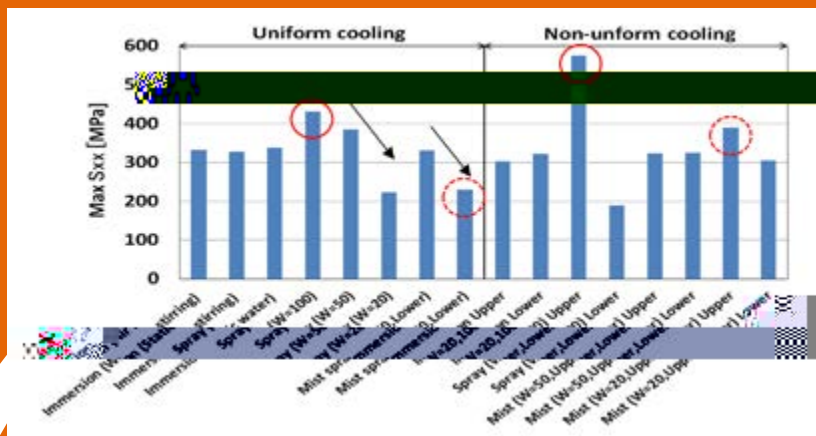


Fig.15 – Max S_{xx} in the case of each cooling method and each cooling condition.

SAMMARY AND CONCLUSION

In this study, the causes of thermal distortion and quenching crack and the effects of kinds of cooling methods and cooling conditions in the reverse transformation treatment were analyzed in order to prevent these troubles by the model of metallo-thermo-mechanics. The cooling methods considered in these analyses were immersion cooling, spray cooling and mist-spray cooling. The fol-

lowing results were obtained from these analyses.

- 1) In several kinds of cooling methods (Immersion cooling, spray cooling and mist-spray cooling) and various cooling conditions, the cooling time required for the reverse transformation treatment were clarified.
- 2) The effects of the cooling methods and various cooling conditions on the cross-sectional shape of the cast bloom after cooling and the stress generated during co-

